



저작자표시-비영리-변경금지 2.0 대한민국

이용자는 아래의 조건을 따르는 경우에 한하여 자유롭게

- 이 저작물을 복제, 배포, 전송, 전시, 공연 및 방송할 수 있습니다.

다음과 같은 조건을 따라야 합니다:



저작자표시. 귀하는 원 저작자를 표시하여야 합니다.



비영리. 귀하는 이 저작물을 영리 목적으로 이용할 수 없습니다.



변경금지. 귀하는 이 저작물을 개작, 변형 또는 가공할 수 없습니다.

- 귀하는, 이 저작물의 재이용이나 배포의 경우, 이 저작물에 적용된 이용허락조건을 명확하게 나타내어야 합니다.
- 저작권자로부터 별도의 허가를 받으면 이러한 조건들은 적용되지 않습니다.

저작권법에 따른 이용자의 권리와 책임은 위의 내용에 의하여 영향을 받지 않습니다.

이것은 [이용허락규약\(Legal Code\)](#)을 이해하기 쉽게 요약한 것입니다.

[Disclaimer](#)



Master Thesis

Analysis of Hot Ductility for Prevention of Edge Crack during Hot-Rolling of Fe-Si steels

Kang, Bong Guk (姜奉局)

Alternative Technology Laboratory
Graduate Institute of Ferrous Technology
Pohang University of Science and Technology

2011



Analysis of Hot Ductility for Prevention of Edge Crack during Hot-Rolling of Fe-Si steels



Analysis of Hot Ductility for Prevention of Edge Crack during Hot Rolling of Fe-Si Steels

by

Kang, Bong Guk

Alternative Technology Laboratory

Graduate Institute of Ferrous Technology

Pohang University of Science and Technology

A thesis submitted to the faculty of Pohang University of Science and Technology in partial fulfillments of the requirements for the degree of Master of Science in the Graduate Institute of Ferrous Technology (Alternative Technology Laboratory)

Pohang, Korea

6, 27, 2011

Approved by

Prof. Koo, Yang Mo

Major Advisor



Analysis of Hot Ductility for Prevention of Edge Crack during Hot Rolling of Fe-Si steels

Kang, Bong Guk

This dissertation is submitted for the degree of Master of Science at the Graduate Institute of Ferrous Technology of Pohang University of Science and Technology. The research reported herein was approved by the committee of Thesis Appraisal

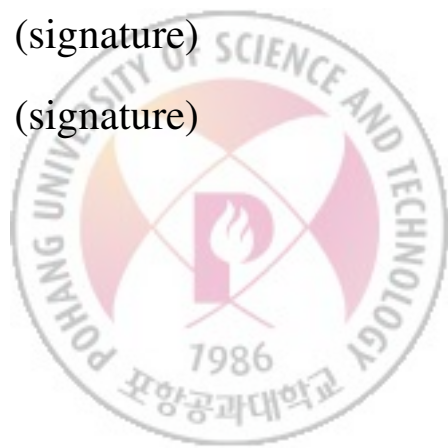
6. 27. 2011

Thesis Review Committee

Chairman : Koo, Yang Mo (signature)

Member : Lee, Jae Sang (signature)

Member : Suh, Dong Woo (signature)



MFT Kang, Bong Guk

20091045

The Analysis of Hot Ductility for Prevention of Edge crack
during Hot Rolling of Fe-Si steels

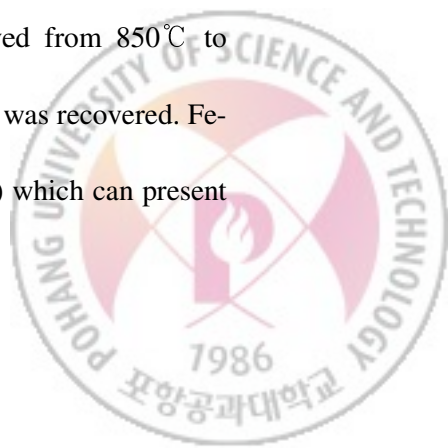
Graduate Institute of Ferrous Technology, 2011

Adviser : Prof. Koo, Yang Mo

Text in English

ABSTRACT

The analysis of the edge crack in the hot-rolled Fe-Si steels ($\text{Si} \leq 1.5$) was carried out by the hot tensile test, examination of the defects, microstructure and finite element method (FEM). The hot ductility of solution treated steels was investigated at temperatures between 800 and 1150°C. Steels were prepared by laboratory vacuum induction melting and then hot rolled into 30-mm-thick plates. Samples for mechanical testing were obtained from hot-rolled plates. Critical transformation temperatures on heating and cooling are also determined using dilatometer. A continuous decrease in ductility was observed from 850°C to about 1000~1050°C in Fe-Si samples. After that, the ductility was recovered. Fe-Si steels have two phase region in high temperature ($\geq 950^\circ\text{C}$) which can present

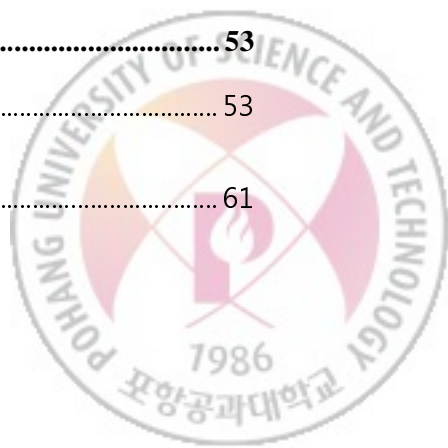


problems during hot-rolling because of reduced hot ductility. The results show that, on cooling, formation of ferrite starts at about 950°C. These results suggest that the low tensile ductility exhibited by these materials at temperatures near 1000~1050°C can be attributed to strain localization at grain boundary nucleated ferrite grains. Rapid growth of microvoids at ferrite films resulted in tensile failure by microvoids coalescence. The results are supported by microstructural observations obtained by electron backscatter diffraction (EBSD) and results of finite element method. The results are also used to discuss the loss of ductility during high temperature deformation of Fe-Si steels and compare to the hot tensile properties of high carbon steel.



Contents

I.	Introduction.....	1
II.	Background.....	3
2.1.	Problems and defects in rolled products	3
2.2.	General description of hot ductility curve	6
2.3.	Influence of Ar_3 and Ae_3 temperature on hot ductility.....	14
2.4.	Effect of test variables on hot ductility	15
III.	Experimental procedure.....	20
3.1.	Experimental	20
3.2.	Methods of hot ductility measurement.....	25
IV.	Result.....	29
4.1.	Dilatometry	29
4.2.	Evaluation of hot ductility.....	32
4.3.	Fractography.....	42
4.4.	Finite element method (FEM) analysis	44
V.	Discussion.....	53
5.1.	Effect of ferrite film on hot ductility.....	53
5.2.	Comparison with high carbon steel.....	61



5.3. Growth of α on γ grain on Fe-Si steel.....	63
5.4. Distribution of temperature and strain during hot rolling	65
VI. Summary and Conclusion	67
Reference	68
Acknowledgements	70
Curriculum Vitae	71



1. Introduction

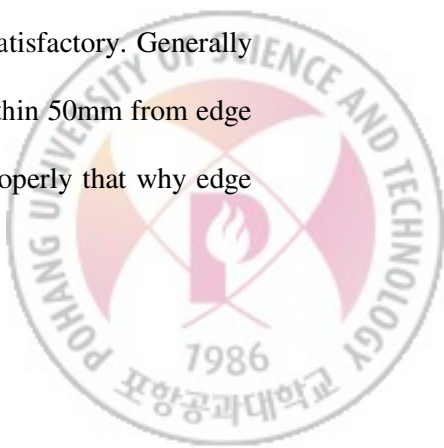
Many edge cracks are often formed along the width direction during hot rolling of Fe-Si steel and high carbon steel. This cracking phenomenon is much severe at surface. Because of these cracks, the value of steel as a product can be decreased and edge cracks can cause a serious deterioration of productivity.

So some researchers attempted to find a mechanism of edge cracks.

In 1998, Jae-Hwa Ryu et al.[1] tried to study the edge cracks phenomenon in hot rolled ultra-low carbon steels. They found that the edge cracks were originated from the abnormal micro-bulging at the bar corner, where ferrite was formed due to the local temperature drop.

In 1999, Myung Hwan Han et al.[2] also tried to investigate the edge cracks phenomenon during hot rolling of non-oriented electrical steel. They showed that appreciable amount of oxides existed inside the surface layer, which might have arisen from the exposure to an oxidation atmosphere. And they explained that because of oxidation occurred on the surface of the edge region along parallel to the rolling direction edge cracks occurred.

However we found that suggested mechanism is no fully satisfactory. Generally edge cracks exist along the rolling direction on the surface within 50mm from edge region. By using their mechanism, it is difficult to explain properly that why edge



cracks occurred along the rolling direction on the surface within that region. Little is known about reason why edge cracks occurred along the rolling direction on the surface.

Some methods to prevent the edge cracking in Fe-Si steel sheets are: (1) refining the microstructure by adjusting the rolling ratio in the roughening mill stand so that the crack growth along the width direction can be prevented [3], (2) edge-rolling at the F0 stand to control the shape of edges[4, 5], (3) pre-rolling of slabs[6], (4) applying an edge heater to prevent super-cooling in the edge region[3]. These methods are usually applied in a combination to solve the edge cracking. However, questions on the effectiveness of these solutions, their applicability to the edge cracking in Fe-Si steel, and the adaptability to the actual rolling conditions remain unanswered.

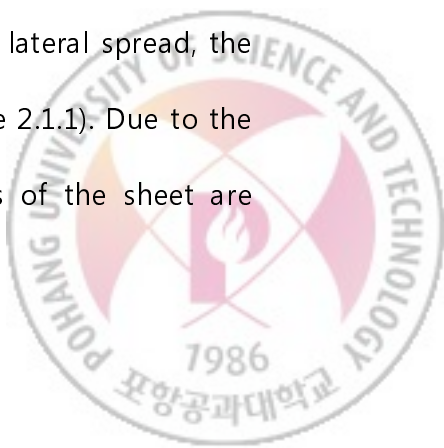
In this reason we tried to find more general relationship between edge crack and hot ductility behavior of Fe-Si steels and compare with the hot tensile properties of high carbon steel in this thesis.



2. Background

2.1. Problems and defects in rolled products

A variety of problems in rolling, leading to specific defects, can arise depending on the interaction of the plastically deformed workpiece with the elastically deforming rolls and rolling mill [7]. Consistent problems with shape and flatness are brought about by inhomogeneities in deformation in the rolling direction of the sheet. Other forms of inhomogeneous deformation can lead to problems with cracking [8]. As the workpiece passes through the rolls all elements across the width experience some tendency to expand laterally (in the transverse direction of the sheet). The tendency for lateral spread is opposed by transverse friction forces. Because of the friction hill, these are higher toward the center of the sheet so that the elements in the central region spread much less than the outer elements near the edge. Because the thickness decrease in the center of the sheet all goes into a length increase, while part of the thickness decrease at the edges goes into lateral spread, the sheet may develop a slight rounding at its ends (figure 2.1.1). Due to the continuity between the edges and center, the edges of the sheet are



strained in tension, a condition which leads to edge cracking (figure 2.1.2). This results in large losses of material because it must be cut off before further processing.

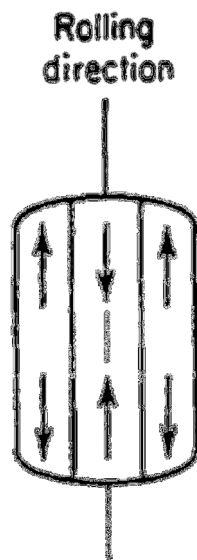


Figure 2.1.1 The shape of sheet during rolling.

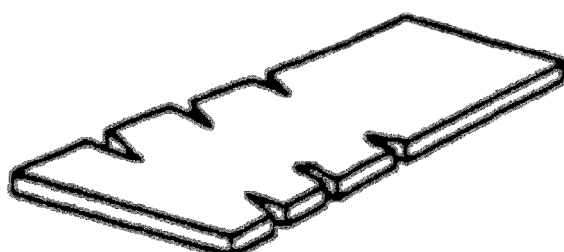
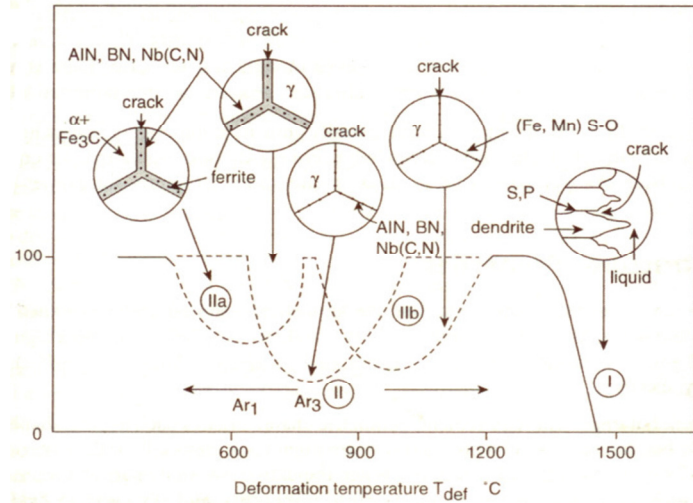


Figure 2.1.2 Defects resulting from lateral spread – edge cracking.

Edge cracking is minimized in commercial rolling practice by employing vertical edge rolls which keep the edges straight and thus prevent a cumulative buildup of secondary tensile stresses due to barreling of the edge. Since most laboratory mills do not have edge rolls, a simple but time-consuming procedure is to equip the mill with edge-restraining bar [9]. Materials with low ductility may be rolled without excessive cracking by "canning" on all sides with a material with a flow stress similar to that of the workpiece. The canning material minimized thermal stresses and provides edge restraint and an increased degree of hydrostatic compression.



2.2. General description of hot ductility curve



I : Liquid \rightarrow Solid transformation

II (a) : Influence of Precipitation

II (b) : Austenite \rightarrow Ferrite Transformation

Figure 2.2.1 Schematic diagram of a hot ductility curve

A typical hot ductility curve for steel is shown schematically in Figure 2.2.1.

The curve contains three general regions, as described by Mintz[10]

- i) HDL region
- ii) Region of embrittlement or trough region
- iii) HDH region

2.2.1. HDL region



One of the essentials in avoiding embrittlement is to reduce the strain concentration at grain boundaries. This concept readily applies to the case of the high ductility, low temperature region.

In the HDL region, which coincides with a relatively high volume fraction of ferrite, the strain is no longer concentrated in a thin ferrite film at austenite grain boundaries. Furthermore, the difference in strength between austenite and ferrite decreases with decreasing temperature, thus increasing plastic strain in the austenite and, more importantly, decreasing the strain in the ferrite[9]. The concentration of strain at the grain boundaries is thus minimized, and high ductility is observed. In ferrite, dynamic recovery, which is a softening process that operates at all strains, readily takes place.

Generally, the ductility is very good when high percentages of ferrite are present in the microstructure, in the vicinity of 700°C. At this temperature, recovery in the ferrite takes place with ease, the subgrain size is large, and the flow stress is low. Thus, ferrite flows readily at triple points to relieve stress concentrations, therefore discouraging the initiation of cracks.

2.2.2. Region of embrittlement



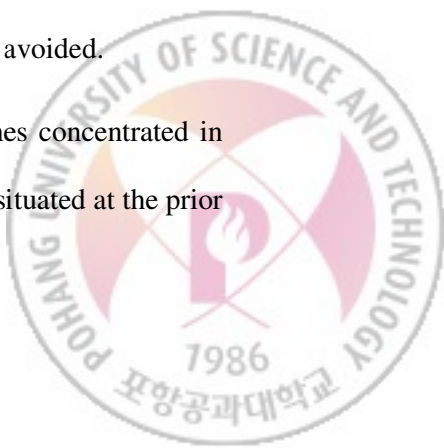
The trough region is invariably associated with intergranular fracture, the fracture facets being either covered with fine dimples or microvoids, or they are smooth, suggesting two distinct mechanisms. In the former case, preferential deformation in regions close to the grain boundary initiates voids at grain boundary inclusions or precipitates which leads to intergranular failure via microvoid coalescence. In the latter case, grain boundary sliding in the single phase austenite region appears to be a viable mechanism.

There are two microstructural features that can be present at austenite grain boundaries and lead to strain concentrations at these locations: (a) thin ferrite films and (b) precipitate free zones.

Ferrite films

Ferrite has excellent hot ductility, but when present as thin bands surrounding coarse γ grains, it gives rise to low ductility intergranular failures in specimens tested in tension at low strain rates. So one of the cracking mechanisms believed to be responsible for the appearance of these cracks is the formation of thin films of ferrite[10]. Hence, an understanding of ferrite formation and of the factors affecting its growth is important if cracking problems are to be avoided.

As ferrite is softer than the γ it surrounds, the strain becomes concentrated in these films. Void formation takes place at the MnS inclusions situated at the prior



γ boundaries and these voids gradually link up to produce ductile intergranular failure.

The thin bands of ferrite that can cause transverse cracking have been shown to form because concurrent straining encourages transformation[11]. Deformation generally raises the Ar_3 temperature applicable to the undeformed material to the vicinity of the Ae_3 temperature. Thus these films are observed over the relatively wide temperature range (about 100°C) stretching from the Ae_3 temperature to the undeformed Ar_3 temperature. Intergranular failure is very common over this range.

When the test temperature is reduced to ~20°C below the undeformed Ar_3 temperature, sufficient ferrite forms before the application of a strain so that the deformation can be accommodated more homogeneously and the ductility recovers.

Much has been learnt in recent years about the formation of such deformation induced ferrite (DIF) in coarse grained materials[12]. Low strain rates are particularly detrimental to the tensile ductility because the ferrite is able to recover and the thin bands remain soft so that the strain is free to concentrate in the boundary regions. Increasing the strain rate is believed to work harden the ferrite at the boundaries so that the strength differential between α and γ phases is reduced. Deformation can then take place in the γ matrix as well as at the boundaries, thus distributing the strain more uniformly. Further deformation then encourages the formation of large quantities of DIF, improving the ductility even

more[12].

Precipitation Free Zones (PFZ)

In Nb containing steels that have been solution treated before cooling to the test temperature, precipitation takes during deformation in the γ . The grain boundary precipitation which usually occurs is frequently accompanied by the formation of relatively weak precipitate free zones (PFZs) on both sides of the boundaries (500nm wide). Fine matrix precipitation can also take place leading to significant matrix strengthening. The situation is then similar to the soft films of deformation induced ferrite and microvoid coalescence fractures are frequently observed. In this case, however, void formation takes place at the microalloy precipitates (Nb(C, N) and AlN when Nb and Al are present together). This fracture process is shown schematically in Figure 2.2.2.1.

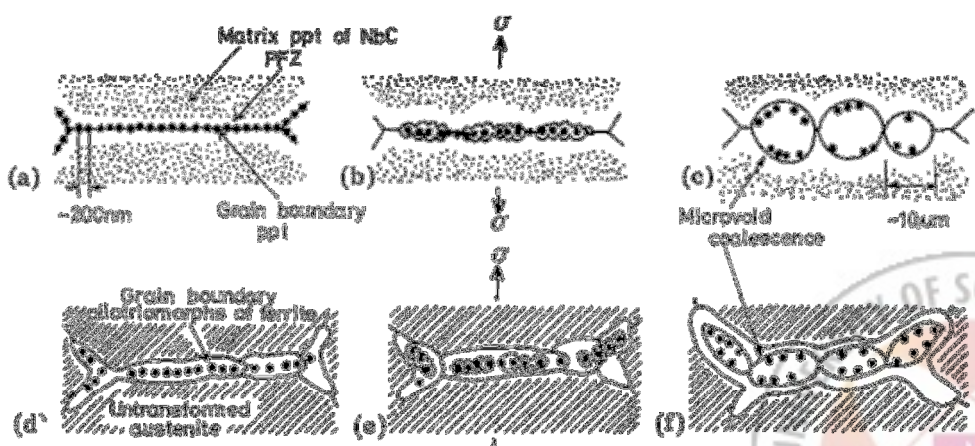


Figure 2.2.2.1 Schematic illustrations showing intergranular microvoid coalescence of niobium-bearing steels by deformation in (a)-(c) the low temperature γ region and (d)-(f) the γ - α duplex phase region.

Grain Boundary Sliding

Grain boundary sliding in the γ leading to the formation of cracks and their propagation, is also a common cause of intergranular failure. This mechanism followed by cracking is seen in γ rather than α because the former show only limited dynamic recovery. This gives rise to high flow stresses and work hardening rates preventing the accommodation by lattice deformation of the stresses built up at triple points or grain boundary particles leading in this way to intergranular failure by the nucleation of grain boundary cracks.

2.2.3. HDH region

On raising the temperature the high ductility, high temperature (HDH) region is encountered. Continuing with the concept of a reduction in the strain concentration at grain boundaries, one obvious reason for this improvement in ductility is the eventual absence of the thin ferrite films. This, of course, is only effective in the austenite plus ferrite two phase region and does not affect the embrittlement in the single phase austenite region which occurs either by grain

boundary sliding or through strain concentration in the PFZ. However, higher temperatures also lead to less precipitation in the matrix and at the grain boundaries, which offsets the latter embrittling mechanisms. Finally increased temperatures lead to lower flow stresses via increased dynamic recovery, which reduce the stress concentrations at the crack nucleation sites.

A further mechanism of ductility increase which applies to the HDH region, but is not based on the concept of reducing the grain boundary strain concentration, requires the occurrence of grain boundary migration. In this case, cracks which have already been initiated are isolated from the prior grain boundaries, and high ductilities result because the growth and coalescence of these cracks is not readily achieved away from grain boundaries. This is evident from the large voids characteristic of the fracture surfaces generated by testing in the HDH region, which apparently are not associated with second phase particles[11]. These grow from the intergranular cracks which form at early stages of the deformation, and which become isolated within the grains as a result of grain boundary migration. The original cracks are then distorted into elongated voids until final failure occurs by necking between these voids.

Although grain boundary migration can isolate cracks from grain boundaries, the cracks can also exert a grain boundary drag force and ‘capture’ moving grain boundaries. Crack growth will then resume along the captured boundary by the combined effects of vacancy diffusion and the applied tensile stress until the boundary breaks away once more. If the capture frequency and/or the crack drag

force are high interfranular failure may ultimately occur even if the prior grain boundaries had moved away from the initiated cracks at an earlier stage in the deformation. Thus, in order to offset embrittlement adequately, the driving force for grain boundary migration must be substantially higher than the drag force exerted by the cracks that are present.

One way to achieve a high driving force for grain boundary migration is by dynamic recrystallization. The nucleation of dynamic recrystallization takes place at existing boundaries at low strain rates[13]. Poorly developed subboundaries pin sections of the original boundaries, which bulge out and migrate relatively rapidly because of the strain energy difference across a given boundary. This is clearly a potent mechanism for bringing about grain boundary movement.



2.3. Influence of Ar_3 and Ae_3 temperature on hot ductility

In 1998, A. Cowley et al. investigated the Influence of Ar_3 and Ae_3 temperature on hot ductility of steel C-Mn-Al, C-Mn-Al-Nb[14].

In his research, they showed that Below the Ae_3 temperature, the troughs were owing to the presence of a thin α film surrounding γ grain. Because strain concentration occurs around MnS inclusions which existed in the α film.

In the case of above the Ae_3 temperature, continuation of the trough was caused by grain boundary sliding in the γ . Recovery of ductility at the high temperature end of the trough corresponded to the onset of dynamic recrystallization and this was delayed in the Nb containing steels so that the trough was extended to higher temperatures. Recovery of ductility at the low temperature end always corresponded to the presence of a large amount of α (~50%) in the structure.



2.4. Effect of test variables on hot ductility

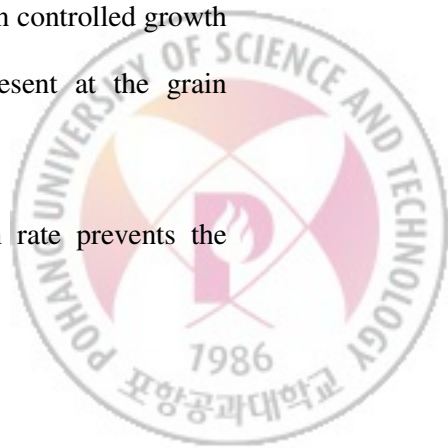
2.4.1. Strain rate

With respect to the range of the strain rates applicable to straightening operations ($\sim 10^{-3}$ - 10^{-4} /s), increasing the strain rate invariably improves the hot ductility, as shown in figure 2.4.1.1 for the strain rate range 10^{-1} - 10^{-4} /s and temperature range 700-1000°C.

This effect can be very marked an increase in strain rate by an order of magnitude often increasing the RA values by ~20%, and changing the fracture appearance from intergranular to ductile. A narrowing of the trough by displacing its upper temperature boundary to lower temperatures is also apparent.

Higher strain rates seem to improve the hot ductility for the following reasons:

1. There is insufficient time for strain induced precipitation.
2. The amount of grain boundary sliding is reduced, i.e. $\varepsilon_g/\varepsilon_t$ decreases as the strain rate is increased, where ε_g is the strain due to grain boundary sliding and ε_t the total strain to fracture[15].
3. There is insufficient time for the formation and diffusion controlled growth of voids next to the precipitates and inclusions present at the grain boundaries.
4. It has also been suggested that increasing the strain rate prevents the



formation of deformation induced ferrite[16].

Decreases in strain rate (e.g. from 10^{-1} to $10^{-2}/s$) have also been shown to improve the hot ductility when unstable fine precipitates such as the FeMn sulphides are present. In this case, the inclusions probably coarsen, so that they are no longer able to pin the γ grain boundaries.

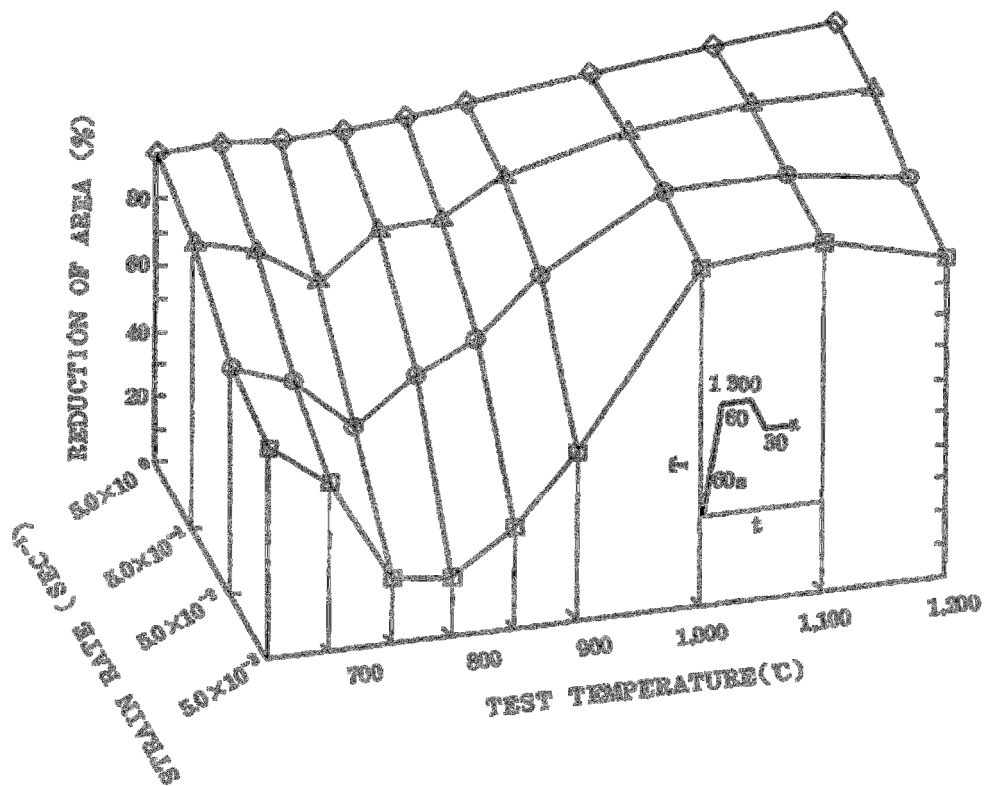
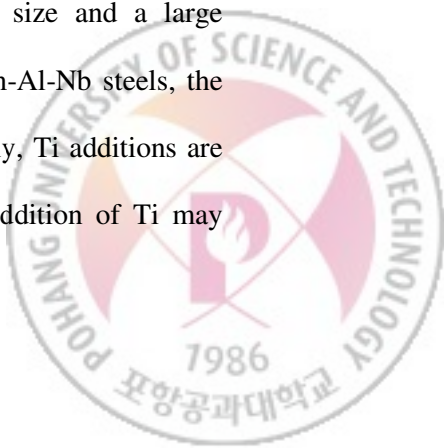


Figure 2.4.1.1 Dependence of ductility on strain rate and test temperature for Nb-bearing steel [17]

2.4.2. Cooling rate

The influence of cooling rate on hot ductility for a wide range of steels has been studied. Generally, Increasing the cooling rate results in lower ductility for most types of steel. In most cases, the decrease in ductility with increasing cooling rate is ascribed to either the formation of a finer particle size or finer inclusion distribution. For C-Mn steels, a finer MnS distribution in the ferrite film surrounding the austenite grains, as well as a reduction in thickness of the ferrite film, can lead to the deterioration in ductility at increased cooling rates. In the case of C-Mn-Al steels, the deterioration in ductility is due to finer AlN precipitation and/or a finer sulphide distribution. For C-Mn-Al-Nb steels, an increase in cooling rate can lead to a greater amount of Nb being held in solution, resulting in an increase in finer, more detrimental, strain-induced Nb(C, N) precipitation. The addition of Ti to Nb containing steels under solution treatment conditions can significantly improve ductility at low cooling rates but little or no improvement is shown at higher cooling rates. At slow cooling rates, the Nb can precipitate out at high temperatures on TiN precipitates, allowing precipitates to coarsen before testing. For solution treatment conditions, TiN precipitates can restrict grain growth in the steel, resulting in finer grain size and a large improvement in ductility. For direct cast C-Mn-Al and C-Mn-Al-Nb steels, the influence of TiN particles on grain size is lost and accordingly, Ti additions are observed to have little influence at any cooling rate. The addition of Ti may



improve ductility by reducing the N available for AlN and Nb(C,N) precipitation.

Ductility is improved due to the reduced volume fraction of precipitation.

2.4.3. Precipitates

In the case of grain boundary sliding in the γ , fine precipitation pins the boundaries, allowing the cracks to join up. In addition both precipitates and inclusions cause void formation, extending the crack length in this way[18]. Microvoid coalescence failures are also encouraged by an increase in the precipitate or inclusion density at the boundaries, these being preferential sites for void initiation.



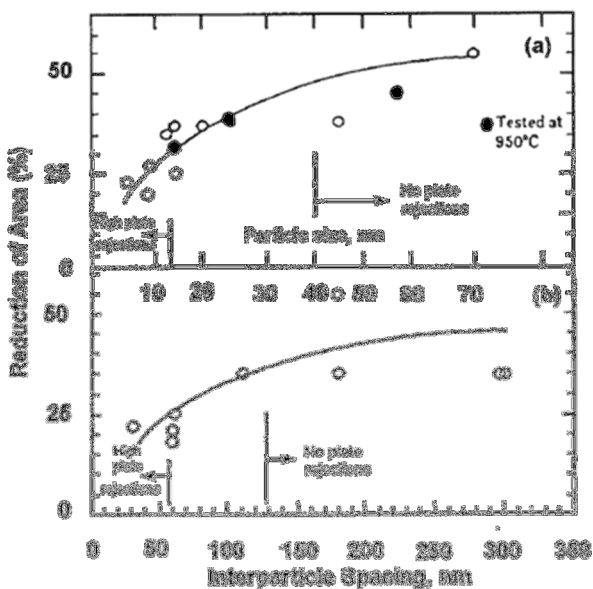


Figure 2.4.3.1 (a) Influence of particle size on hot ductility

(b) Influence of interparticle spacing on hot ductility[10]

There is a large body of evidence which indicates that low RA values in common microalloyed steels are associated with fine precipitation. It is also generally accepted that it is the precipitation at the γ boundaries that has the greatest influence. This is clear in figure 2.4.3.1, where the influence of the Nb(C, N) precipitates at the γ grain boundaries on the hot ductility of C-Mn-Nb-Al steels is shown, for the rare instance where all the other variables have been kept reasonably constant. Also included in this figure are the results from a commercial examination into the precipitate distributions at the γ grain boundaries.

3. Experimental procedure

3.1. Experimental

Fe-Si steel and high carbon steel were prepared by vacuum induction melting and then hot rolled into 35-mm-thick plates. The chemical compositions of the steels are listed in Table 1.

Steel	C	Si	Mn	P	S	Al	N	Cr	V
A	0.005	0.861	0.167	0.023	0.005	0.120	0.0018	-	-
B	0.003	1.231	0.155	0.012	0.002	0.380	0.0018	0.010	0.001
C	0.519	0.218	0.881	0.013	0.002	0.012	0.0042	1.093	0.102

Table 3.1 Chemical composition of Fe-Si steels and high carbon steel (wt%)

High temperature tensile test specimens were machined from the plate in the longitudinal axes parallel to the rolling direction.

The reduction of area (RA) was measured to evaluate the hot ductility of steel. And Elongation was also measured to compare with reduction of area. Measurement of RA and Elongation curves as a deformation temperature is very useful to describe surface cracking during hot-rolling process. High temperature

tensile tests were conducted using a thermo mechanical simulator with dilatometer, figure 3.1.1.

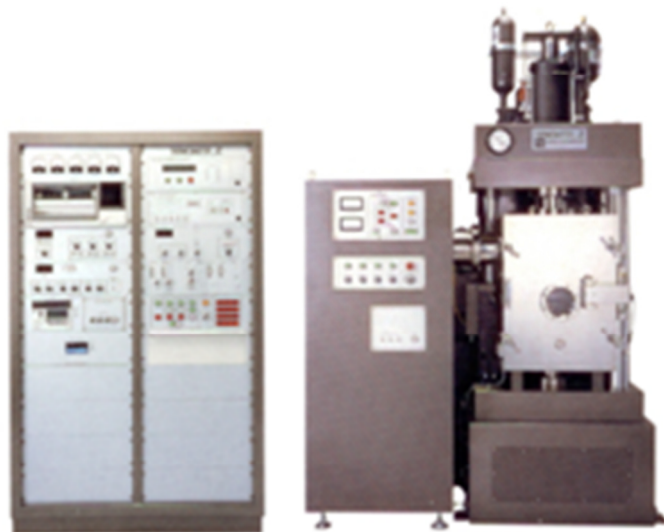


Figure 3.1.1 Thermo mechanical simulator

Specimens were heated by high frequency induction. The specimens were 5mm in diameter and had gauge length of 10mm, Figure 3.1.2.



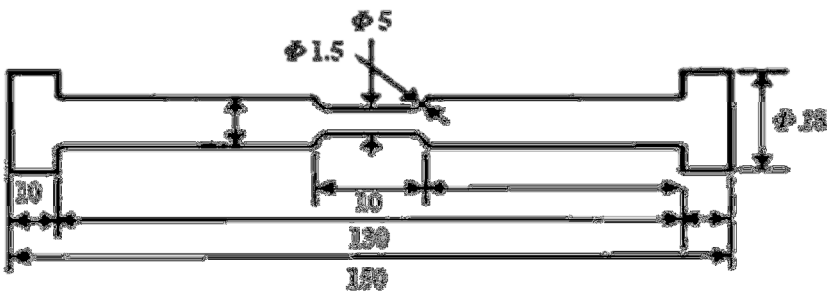


Figure 3.1.2. Shape of the high temperature tensile test specimen of Fe-Si steel

Figure 3.1.3 shows the thermal cycle of the high temperature tensile test. The specimens were heated from room temperature to 1200°C at 10°C/s, held for 10 minutes to allow microstructural homogenization and then cooled to the deformation temperature (600 to 1150°C) at cooling rate of 2°C/s which is actual cooling rate at edge part during hot-rolling process. Specimens were held at the test temperature for 5 seconds and then strained to failure at a strain rate of 5×10^{-3} , 10^{-1} /s to investigate effect of strain rate during tensile test. In addition, to investigate the effect of hold-time, high temperature tensile test was conducted at different hold-time after cooling until deformation temperature. And also high temperature tensile test was conducted at deformation temperature during heating. To minimize oxidation, all strain tests were conducted in an inert atmosphere of Argon gas. Also, some samples were directly quenched by water spraying to preserve the proeutectoid α and γ . Sections parallel to the tensile axis were prepared

for metallographic. And then an etchant used for revealing prior γ grain boundaries by A. Brownrigg et al. was tried[19]. The etchant is 100ml saturated aqueous picric acid + 2ml “Teepol” + 6 drops of concentrated HCl. And 2% nital is also used. The microstructures of the specimens were examined using an optical microscope and the fracture surface of the specimen was examined using SEM.

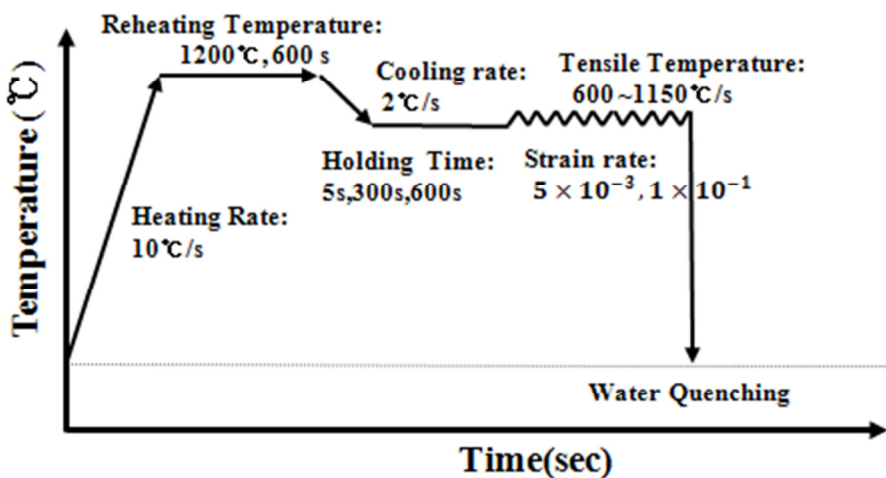


Figure 3.1.3 Thermal cycle of high temperature tensile test

The equilibrium temperature of γ/α phase boundary (Ae_3) calculated using Thermo-Calc (Thermo Calc software, Inc.) was about 1013°C (steel A), which indicated that proeutectoid α was no formed above 1100°C in these steels. And also the Thermo-Calc program was used to calculate the volume fraction of α which would be present under equilibrium conditions.

Dilatometry was carried out on this steel on specimens given the same preheat

treatment and cooled at 2°C/s to room temperature.



3.2. Methods of hot ductility measurement

3.2.1. Reduction of area

RA value has been a most popular method for representing hot-ductility.

Reduction of area was calculated as follows:

Percent reduction of area (RA) =

$$\frac{\text{area of original cross section} - \text{minimum final area}}{\text{area of original area}}$$

$$= \frac{A_0 - A_{min}}{A_0} = \frac{\text{decrease in area}}{\text{original area}} \times 100$$

Many of researchers have used RA value, for measuring ductility of materials. The RA value required to prevent edge cracking from occurring is dependent on test variables.

The influence of high hot ductility values on the control and elimination of cracking was studied in high temperature tensile test as a means of determining measures for hot rolling process. According to Kawasaki et al.[20], Sheet bar samples obtained at the roughing mill with RA's higher than 70% did not crack at the finishing mill; on the contrary, however, those with RA's below 70% showed edge cracks of about 5mm.

In the case of continuous casting process, transverse cracking is almost observed

under 30% of RA value[21].

3.2.2. Elongation

Elongation is one of the most popular test to measure the ductility of material.

When a material is tested for tensile strength it elongates a certain amount before fracture takes place. The two pieces are placed together and the amount of extension is measured against marks made before the test and is expressed as a percentage of the original gauge length.

The percent elongation reported in a tensile test is defined as the maximum elongation of the gauge length divided by the original gauge length. The measurement is determined as shown in figure 3.2.2.1.

Percent elongation =

$$\frac{\text{final gauge length} - \text{initial gauge length}}{\text{initial gauge length}}$$

$$= \frac{L_f - L_0}{L_0} \times 100$$



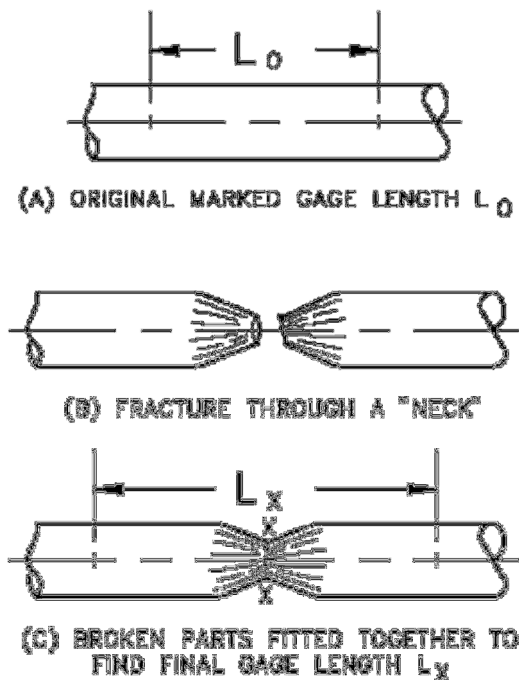


Figure 3.2.2.1. Measuring elongation after fracture

The RA is reported as additional information (to the percent elongation) on the deformational characteristics of the material. The two are used as indicators of ductility, the ability of a material to be elongated in tension. Because the elongation is not uniform over the entire gauge length and is greatest at the center of the neck, the percent elongation is not an absolute measure of ductility. (Because of this, the gauge length must always be stated when the percent elongation is reported.) The RA, being measured at the minimum diameter of the neck, is a better indicator of ductility.

Ductility is more commonly defined as the ability of a material to deform

easily upon the application of a tensile force, or as the ability of a material to withstand plastic deformation without rupture. Ductility may also be thought of in terms of bendability and crushability. Ductile materials show large deformation before fracture. The lack of ductility is often termed brittleness. Usually, if two materials have the same strength and hardness, the one that has the higher ductility is more desirable. The ductility of many metals can change if conditions are altered.



4. Result

4.1. Dilatometry

Figure 4.1.1 shows the dilatation curves for Fe-Si steel and high carbon steel. On heating, transformation from the initial state of ferrite to austenite, as indicated by a decrease in the slope of the length-temperature trace, began at about 1020°C for Fe-Si steel and was completed at about 1050°C for Fe-Si steel. Similar remarks apply to the transformation of $\gamma \rightarrow \alpha$ on cooling where the start of transformation was estimated to be 954°C for Fe-Si steel after reheating at 1200°C. Transformation behavior of Fe-Si by dilatometry shows that the steel has high transformation temperatures for the $\gamma \leftrightarrow \alpha$ phase transformation on both heating and cooling.

The calculated Ae_3 (from the Thermo-Calc) and experimentally determined Ar_3 temperatures are listed in Table 2.

Steel	Ae_3	Ar_3
A	1013°C	954°C

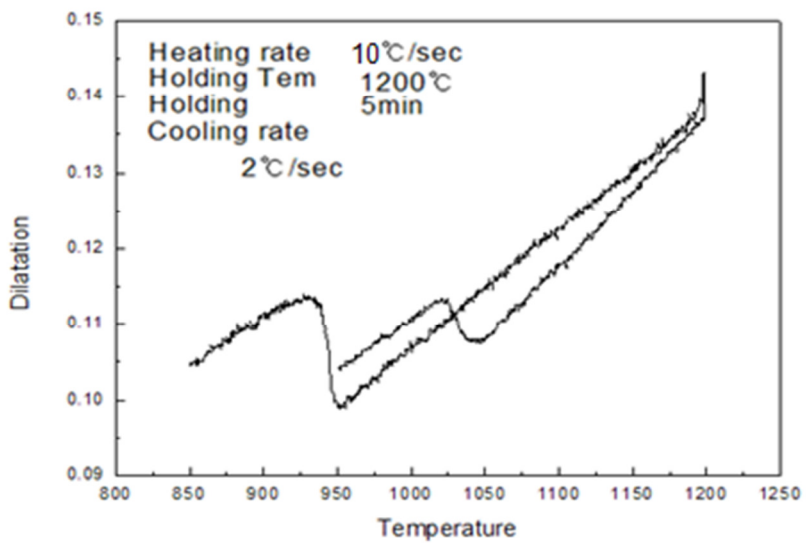
Table 2. Transformation temperature of the steel A (°C)

Ae_3 : Calculated by using Thermo-Calc program

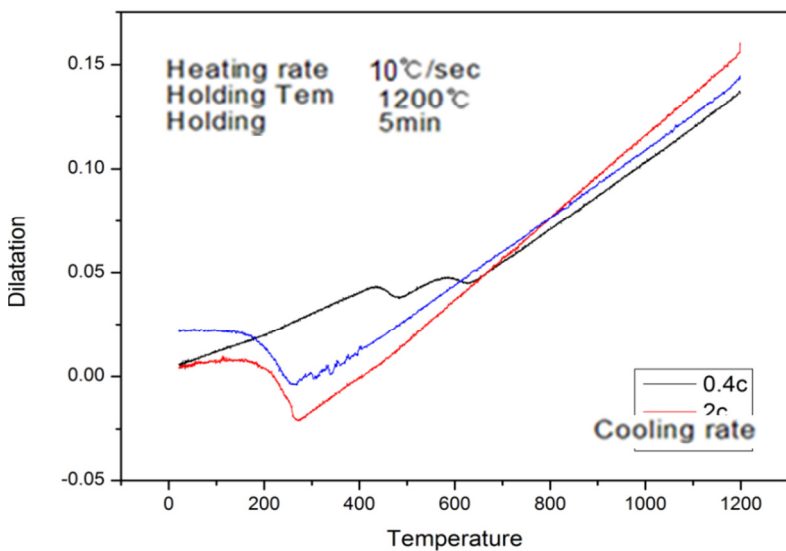
Ar_3 : Measured by dilatometer; the specimens were cooled continuously at a rate of 2°C/s after heating at 1200°C

In the case of high carbon steel, however, $\gamma \leftrightarrow \alpha$ phase transformation can't be observed by dilatation test, because of very small fraction of ferrite surrounding austenite grain boundaries. Instead of this, large amount of perlite transformation started at 653°C for 0.4°C/s cooling. Over 2°C/s cooling rate, martensite transformation was observed at 270°C. It is very different to Fe-Si steels transformation.



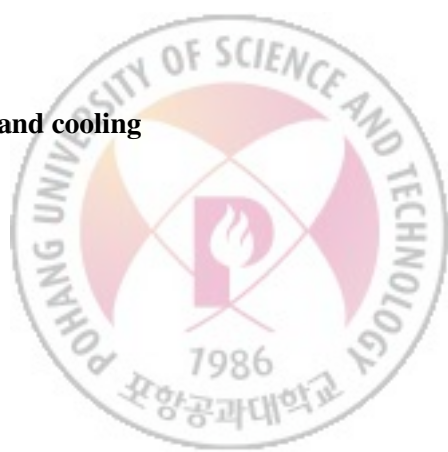


(a) steel A



(b) Steel C

Figure 4.1.1 Dilatation curve of steel A, C during heating and cooling



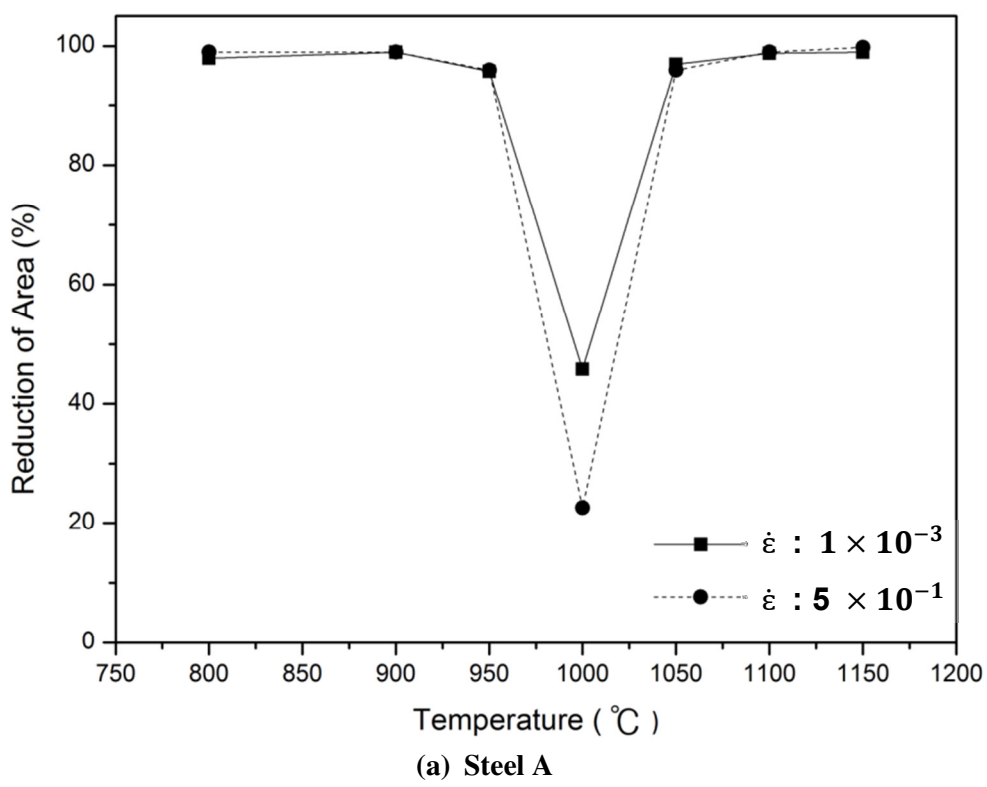
4.2. Evaluation of hot ductility

4.2.1. The effect of strain rate

The steels can be seen to have different hot ductility curves in figure 4.2.1.1. In Fe-Si steel, the ductility trough occurred between 950°C and 1050°C with the minimum ductility at 1000°C. The effect of strain rate on ductility curve is not significant in this steel. Minimum ductility temperatures range of Fe-Si was significantly higher than that usually observed in plain C-Mn, C-Mn-Al or microalloyed steels (generally below 800°C) [10]. The ductility was recovered at the highest and lowest temperatures. The improvement in ductility at the low temperature end of the hot ductility in steels tested at low strain rates, always corresponds to the presence of a significant volume fraction of ferrite; ferrite having excellent ductility. Thus processes at lower temperatures when a significant amount of ferrite is present can give excellent ductility, more than enough to prevent cracking. In high carbon steel, the ductility trough cannot observe at 1×10^{-1} strain rate. However, decreasing strain rate caused the ductility trough between 600°C and 750°C. The minimum ductility for high carbon steel occurs at 650°C. Transformation start temperature (Ae_3) calculated using Thermo-Calc was 755°C in this steel. Generally, at temperatures slightly below Ae_3 temperatures, proeutectoid ferrite occurs as thin layers along austenite grain boundaries. If stress is applied to this microstructure, the strain concentrates within these soft ferrite

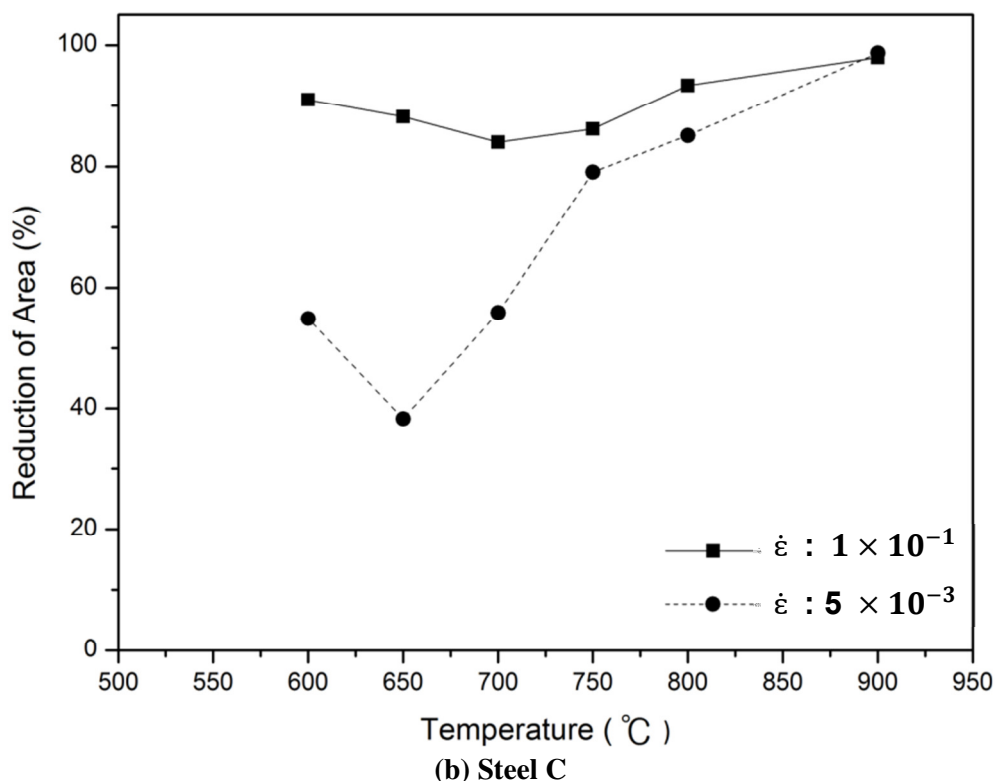
layers[22]. Therefore the steel's ductility is lower than that of any other temperature. In the high carbon steel, a more severe drop in ductility around Ae_3 at 5×10^{-3} strain rate than did at 1×10^{-1} strain rate. Because of higher strain rate, there is insufficient time for concentration of stress at ferrite films.





(a) Steel A





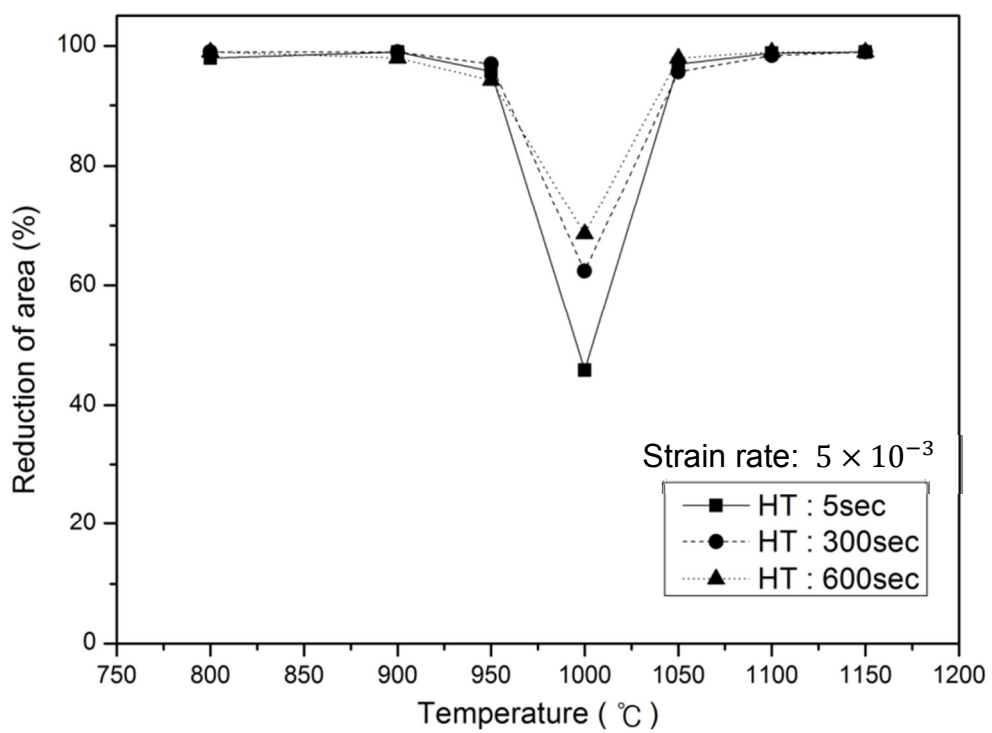
$\dot{\varepsilon}$: Strain rate

Figure 4.2.1.1 Hot ductility curves for steel A (a), steel C (b) with different strain rate

4.2.2. The effect of holding-time

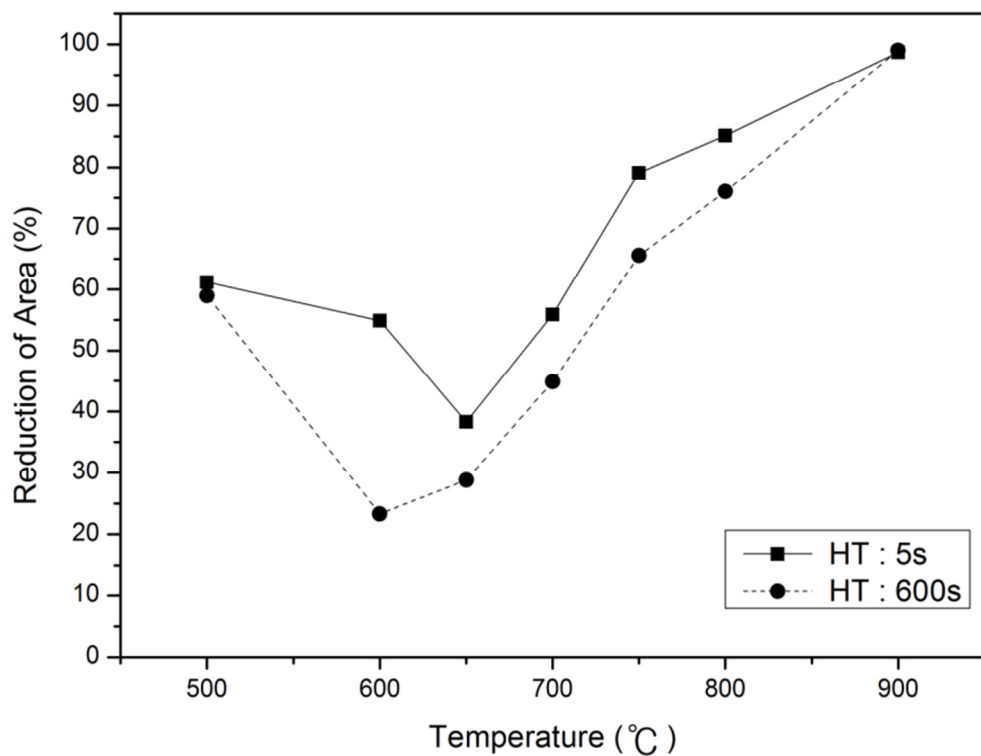
Figure 4.2.2.2 shows that the hot ductility curves measured during different holding-time after cooling until deformation temperature to investigate effect of hold-time. In the Fe-Si steel (steel A), Minimum ductility has been observed in the same temperature (1000°C) in spite of increasing holding time. Minimum RA values of Fe-Si steel, however, are increasing as increasing holding time. Generally, ferrite grain growth occurred during increasing holding-time. Therefore, hot ductility is improved. In the high carbon steel, ductility values of 600s holding time were similar to values of 5s holding time at 5×10^{-3} strain rate. Because time for phase transformation was enough at slower cooling rate.





(a) Steel A





(a) Steel C

Figure 4.2.2.2 Hot ductility curves for steel A (a), steel C (b) with different holding-time



4.2.3. Ductility curve of silicon steels

Figure 4.2.2.3 shows that the hot ductility curves for steel A, B with 0.1/s strain rate. It is difficult to measure RA values because the fracture surface of steel B is not clear. So elongation values are used in this test. The temperature of minimum ductility is 1000°C which is just below Ae_3 temperature in steel A. In the case of steel B, relatively low ductility values are measured over 1100°C which is in two phase region. Therefor ferrite film must have affected hot ductility behavior of silicon steels.

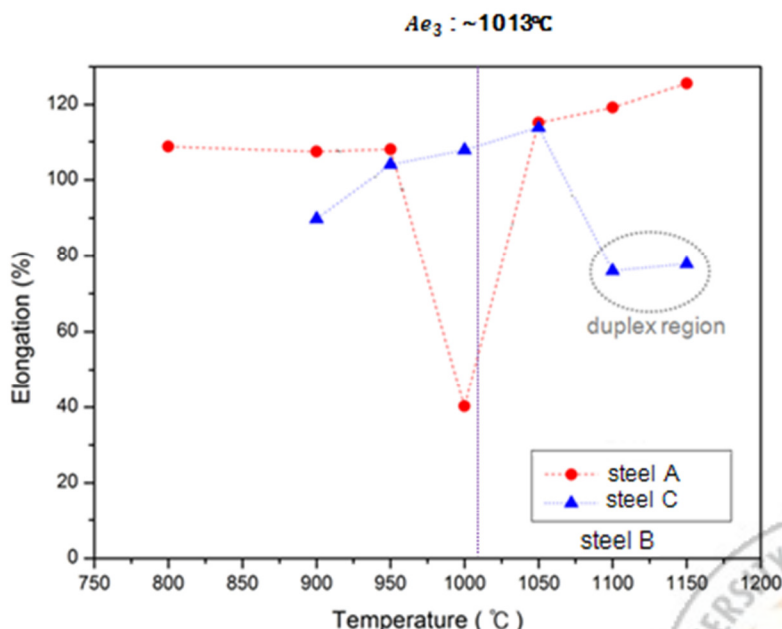


Figure 4.2.2.3 Hot ductility curves for steel A, steel B with 0.1/s strain rate

4.2.4. Hot ductility during heating

Figure 4.2.2.4 shows that the hot ductility curves of Fe-Si steel (steel A) measured by reduction of area during cooling and heating. The positions of the troughs were different for cooling and heating. Minimum ductility occurred at 1000°C during cooling process. And at 1050°C, hot ductility was recovered and shows over 90% RA value.

On the other hand, minimum ductility occurred at 1050°C during heating process. And at 1100°C, hot ductility was recovered and shows about 90% RA value.

Figure 4.2.2.4 and figure 4.1.1 (a) indicate that ductility troughs corresponded to the end of phase transformation (Figure 4.1.1 (a)) during cooling and heating in both cases. This result can be explained by thin ferrite on the austenite boundaries.



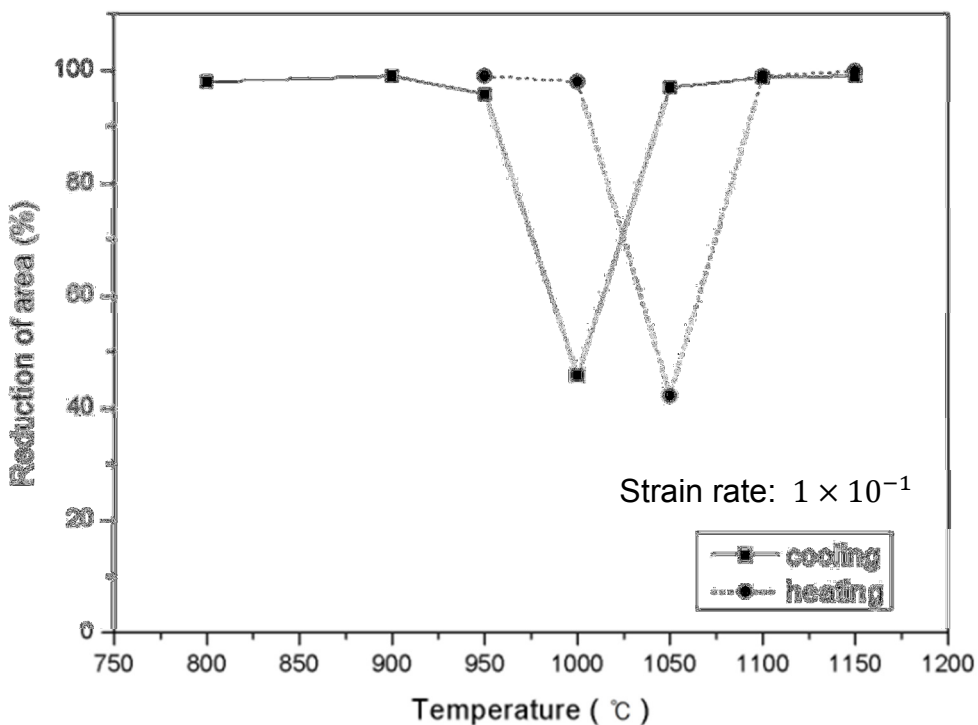


Figure 4.2.2.4 RA curves for Fe-Si steel (steel A) during cooling and heating

process.



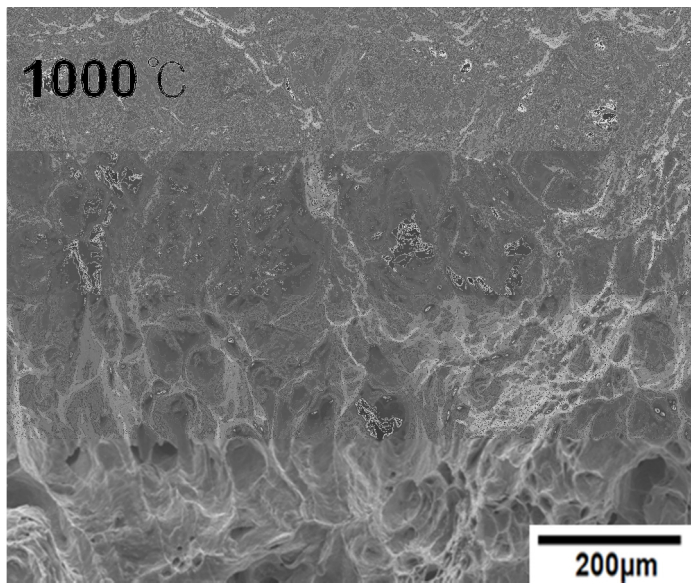
4.3. Fractography

Figure 4.3.1 shows that ductile fracture occurred at 1000°C (steel A) and 650°C (steel C) which were the lowest R of A value, respectively. Intergranular cracks are usually observed along austenite grain boundaries in low C steels. The mechanisms of intergranular cracking of low C steels deformed at high temperatures have been associated with the formation of ferrite films (5~20 μm thickness) induced by deformation concentrations to temperatures slightly below the Ae3 temperature on the austenite grain boundaries[12]. In this Fe-Si steel, however, evidences of intergranular cracks and ferrite films on the austenite grain boundaries are not found through the micrographs because of massive ferrite transformation.

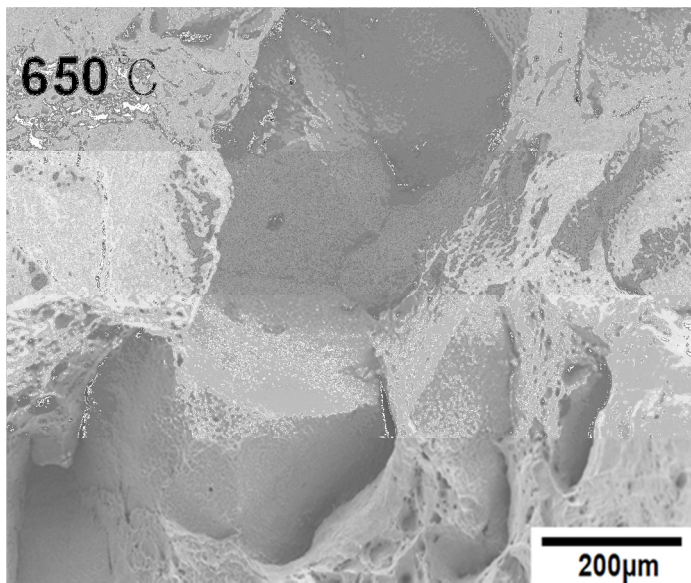
Ductile fracture of surface which is occurred at under the Ae3 temperature indicates that this Fe-Si steel measured has a better ductility than low C steels. But cracks can be occurred in this steel because ductility is a relative value.

In the case of high carbon steel, on the other hand, completely intergranular fracture mode was shown in figure 4.3.1 (b). Intergranular fracture with apparent grain boundary facets is characteristic fracture mode in that temperature range (650~700°C), which shows the smallest RA value.





(a) Steel A



(b) Steel C

Figure 4.3.1 SEM micrographs, showing surface fracture by high temperature tensile test in steel A and steel C.

4.4. Finite element method (FEM) analysis

In order to investigate distribution of strain and temperature in actual process, FEM was performed by means of commercial and professional plastic forming software DEFORM-3D. In the current simulation, the coordinates system was set as that the perpendicular direction as the z-axis and the other two as the x-axis and y-axis, respectively.

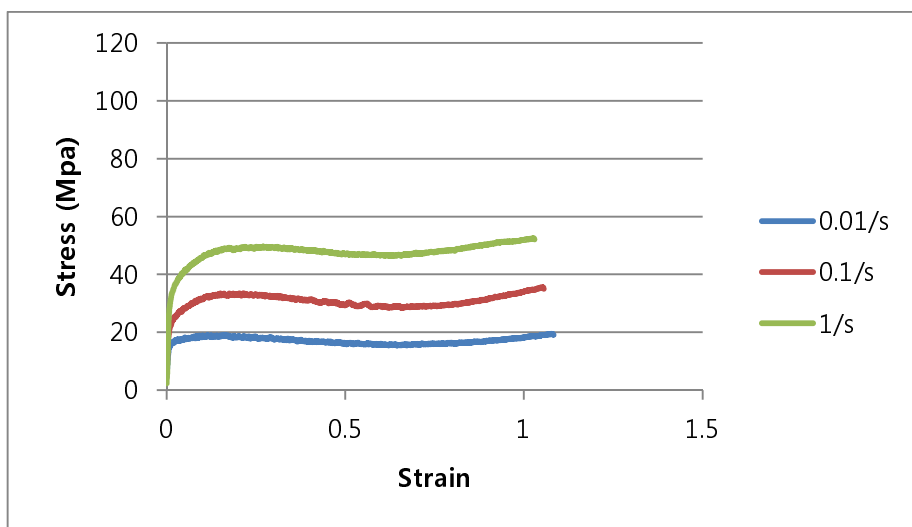
- (1) During the hot-rolling process, the upper roll and the down roll, which were the main modules with a given rolling speed (Table 4) along the rotation axis, x-axis.
- (2) It cost about 27s to fetch the strip from the furnace onto the roll. Though this time-interval was shorter, the strip would have a larger value of temperature drop since that was very hot, so it needed to be taken into account.

The other simulation parameters are shown in Table 1, simulation conditions (roughing mill) are shown in Table 2. And the data of compression test used for calculation are shown in figure 4.4.1

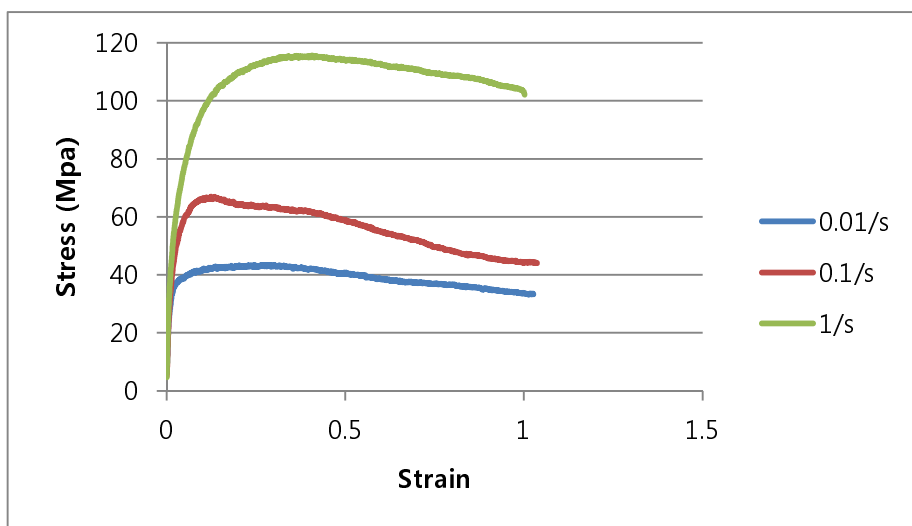
In order to ensure that the simulation agrees with the actual hot-rolling process as possible, this process was divided into three stages: (1) from the strip being taken out of the furnace to contacting with rollers; (2) from the strip contacting with the rollers to its rolling begins; (3) interpass time. In addition, actual

roughing mill conditions were used through the entire hot-rolling process, to ensure the accuracy of the simulation.



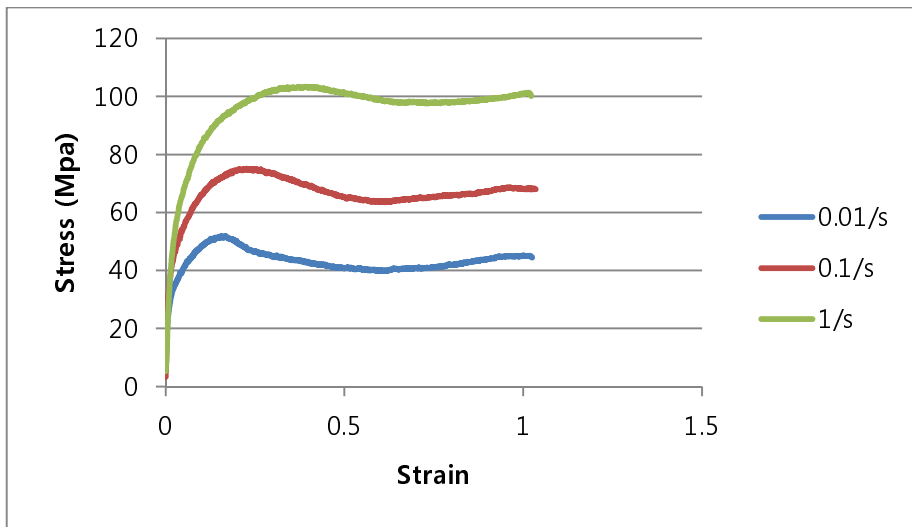


(a) 950°C

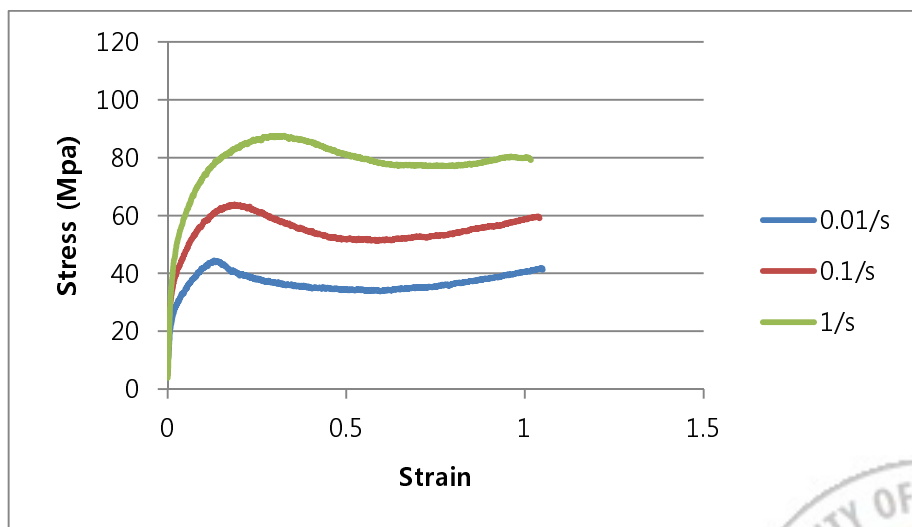


(b) 1000°C

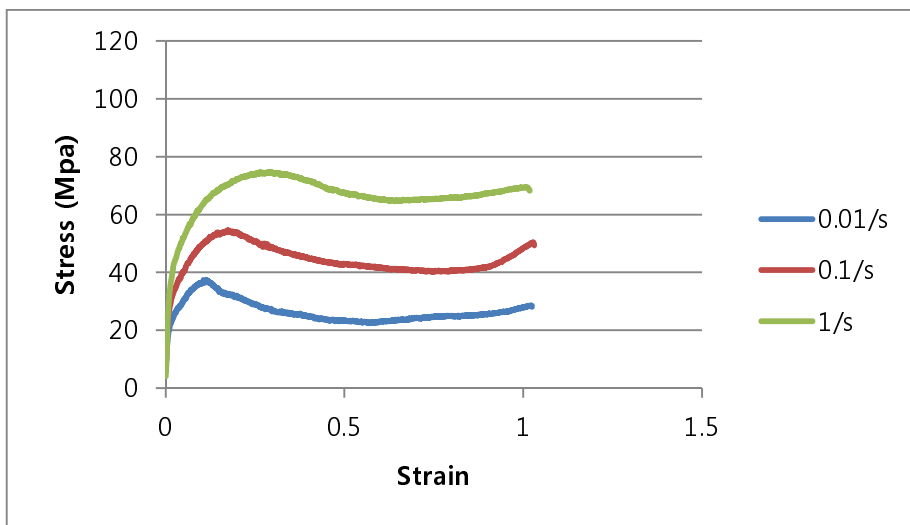




(c) 1050°C



(d) 1100°C



(e) 1150°C

Figure 4.4.1 Strain stress curves of steel A at different test temperatures which are used for FEM



Simulation parameters	Values
Length of strip (mm)	700
Height of strip (mm)	253
Mesh number of strip	5,400
Initial temperature of strip (°C)	1250
Fraction factor	0.7

Table 3. Simulation parameters

		R1					R2				
		1pass	2pass	3pass	4pass	5pass	6pass	7pass	8pass	9pass	10pass
Condition	Thickness (mm)	227	188	153			125	102	81	66	52
	Reduction rate (%)	10.3	17.2	18.6			18.3	18.4	20.6	18.5	21.2
	Speed [m/min]	140	160	176			210	210	220	220	220
	Work Roll Dia (mm)	1288					924				

Table 4. Simulation conditions



During whole process, the thermal loss of the strip is shown in figure 4.4.2. The heat drop of the edge surface of strip is significantly higher than the center surface of the strip by 100°C. The temperature of point 1 (edge) is decreased until 1010°C during the entire process.

To further understand the changes of the temperatures, stresses and strains at different parts of the strip during the whole hot-rolling process, chose four representative points form the deformed strip. And the temperature change of these four points in the entire hot-rolling process is shown in left-down corner of the figure 4.4.2.

This graph shows that the temperature change gradient of point 1 (edge) is much higher than that of point 2, 3 and 4 (center) during the entire hot-rolling process.

Figure 4.4.3 shows the strain distribution on the surface of strip along x-axis and the four points during the entire hot-rolling process. From this graph can clearly see that the strain of point 1 (edge) remarkably larger than at points 2, 3 and 4 (center). And strain curves at point 2 and 3 are similar.



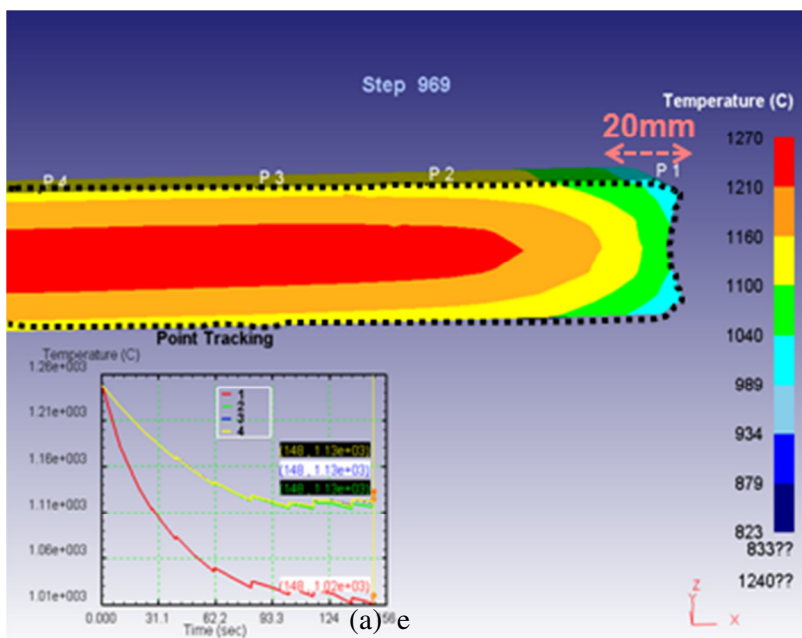


Figure 4.4.2 The predicted temperature distribution within the rolling metal of steel A (1. Edge; 4. Center).

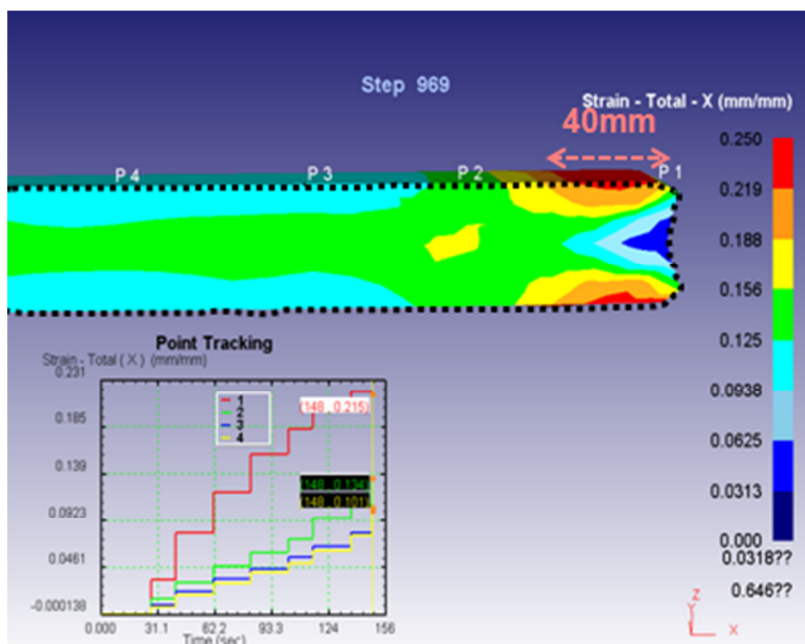


Figure 4.4.3 The predicted strain distribution within the rolling metal of steel A (1. Edge; 4. Center).

5. Discussion

5.1. Effect of ferrite film on hot ductility

Figure 5.1.1 shows that the Fe-Si-Mn-Al phase diagram calculated by Thermo-Calc. In this figure, the thermodynamic simulations were carried out by chemical compositions of Table 1. The dotted line expresses the contents of silicon. The equilibrium temperature Ae_3 is 1013°C in Fe-Si steel. The Ae_3 temperatures determined by Thermo-Calc correspond to undeformed austenite. Although Ar_3 temperature is lower than Ae_3 temperatures, the measured temperatures can be taken as an estimation of the maximum temperature at which proeutectoid ferrite can be expected to form from deformed austenite during hot rolling process. Normally, poor ductility can be explained by precipitate and ferrite film on the austenite grain boundaries. In these steels, Precipitates such as AlN does not occur. Reduced ductility during phase transformation can be explained by figure 4.2.2.3. Ductility is also decreased at just below the transformation temperature during heating process. Thus formation of proeutectoid ferrite films around the prior austenite grain boundaries during hot deformation can account for the decreased ductility. Concentration of plastic deformation occurs in this region due to the low resistance of ferrite, causing rapid coalescence of microcavities at the austenite/ferrite interface. Poor ductility is caused by deformation between the austenite and ferrite phases due to their strength difference at a given temperature.

That is, the primary factor controlling hot ductility in the austenite/ferrite region is the thickness of the ferrite layer (or volume fraction of ferrite).



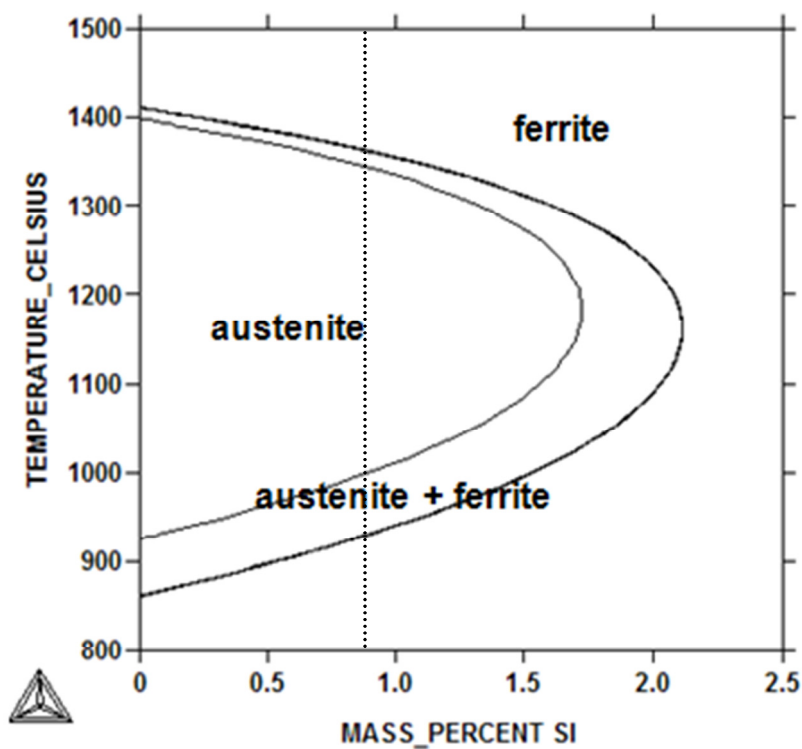
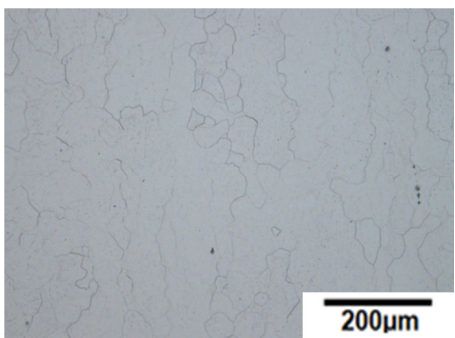


Figure 5.1.1 Fe-Si-Mn-Al phase diagram calculated with Thermo-Calc
for chemical composition of steel A

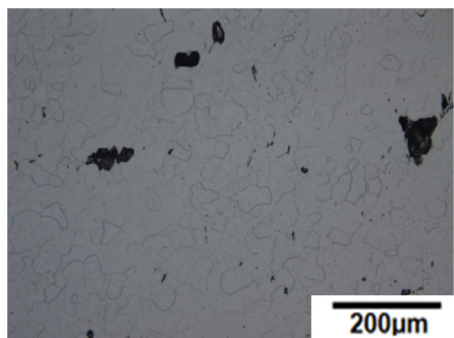
Hot rolling of Fe-Si steels is usually performed at temperatures between 1200°C and 800°C. Thus, the presence of ferrite during hot rolling is unavoidable and the results presented in this work indicate that these materials are highly susceptible to intergranular cracking during processing.

Several hot deformation mechanisms for intergranular fracture at the higher temperature have been proposed. They are related to the hot deformation mechanisms such as dynamic recrystallization[23],[15] or grain boundary sliding[10], both of which are strain-rate dependent processes. Therefore the effect of strain rate on hot ductility was investigated in the high carbon steel. As shown in figure 4.2.2.1, RA values were widely changed, especially at a range between 600°C ~750°C. Hot ductility of the high carbon steel was improved with increase of strain rate, but the temperature of the minimum of the ductility trough did not change. The improvement of hot ductility in this region with the increase of strain rate indicates that it represses strain concentration in ferrite grain during deformation, resulting in homogeneous deformation in both austenite and ferrite phase.

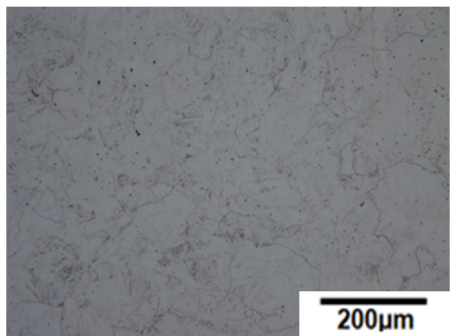




(a) 900 °C



(b) 650 °C



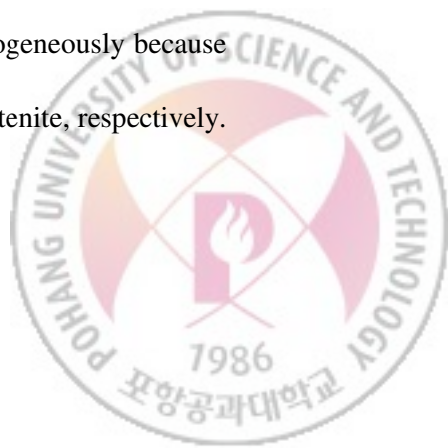
(c) 1000 °C

Figure 5.1.2 Room temperature microstructure of steel A cooled from 1200 °C to the deformation temperatures, held during 5s, deformation ($\dot{\varepsilon}=5 \times 10^{-3}$) and finally quenched.

Longitudinal cross-sectional microstructures were obtained near the fractured surfaces of Fe-Si steel and high carbons steel, which had been cooled at 2°C/s cooling rate at each deformation temperature.

Figure 5.1.2 shows that microstructures of Fe-Si steel after deformation. On etching the deformed Fe –Si specimens in 100ml saturated aqueous picric acid + 2ml “Teepol” + 6 drops of concentrated HCl, the structures obtained in Fe-Si steel were only ferrite for the three deformation temperatures used. As shown in figure 5.1.2 (a) almost ferrite grains were deformed severely and the grain boundaries more irregular for the 900°C (ferrite region) deformation temperature. And recrystallization occurred at some ferrite grains. At 1000°C (figure 5.1.2 (b)) which is two phase (ferrite + austenite) region slightly below the Ae_3 temperature, the microstructure exhibit mainly polygonal ferrite. Generally, thin film of proeutectoid ferrite was presented at austenite grain boundary slightly below the Ae_3 temperature. But in this case thin ferrite file did not present. And also lots of internal cracks occurred in the figure 5.1.2 (b). At 1150°C (austenite region), Polygonal ferrite and bainitic ferrite was presented.

The image quality (IQ) maps of microstructures steel A at different temperatures (a) 900°C, (b) 1000°C, (c) 1150°C, respectively, are shown in figure 5.1.3. At 900 and 1150°C, Strain is distributed at almost ferrite grains homogeneously because these temperatures are a single phase region, (a) ferrite (c) austenite, respectively. In the case of (b) 1000°C



, however, strain is distributed at the specific ferrite grains. It is evident that two phase ($\alpha+\gamma$) existed at this temperature. When the strain is increased, film like ferrite grains exist at around austenite grain boundary at 1000°C. Therefore strain is almost concentrated on the specific ferrite grains. These grains are marked as the red grains in this figure (b).



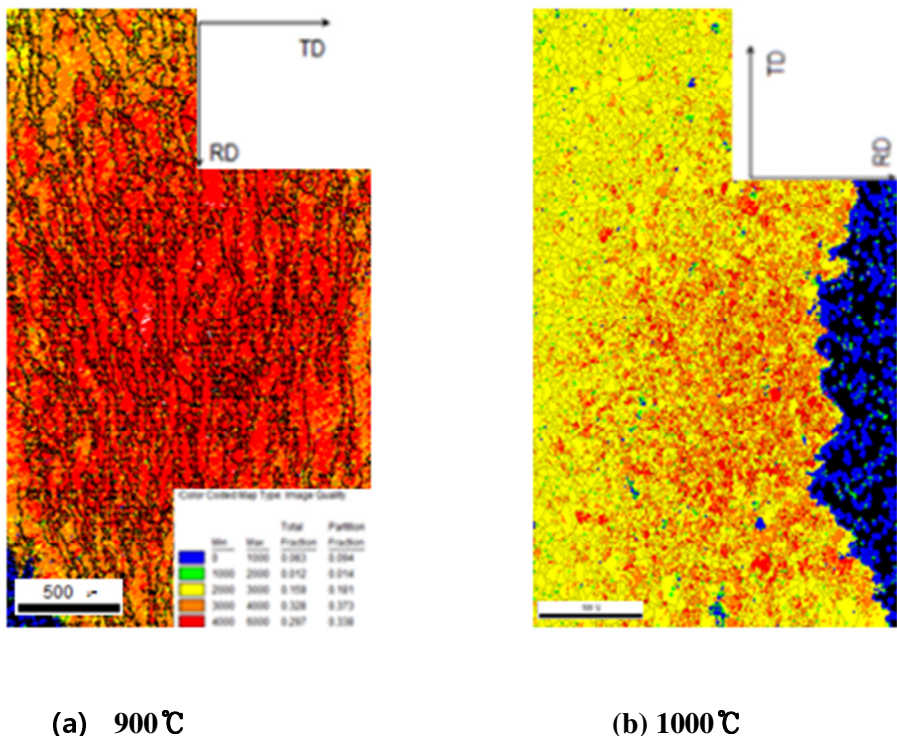
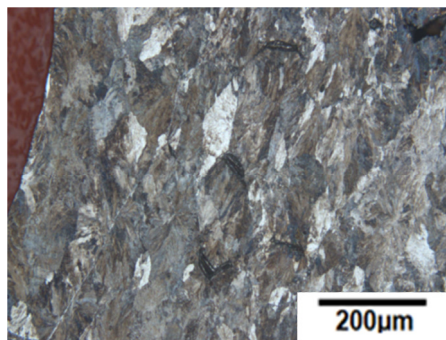


Figure 5.1.3 Image quality maps of steel A at different test temperature.

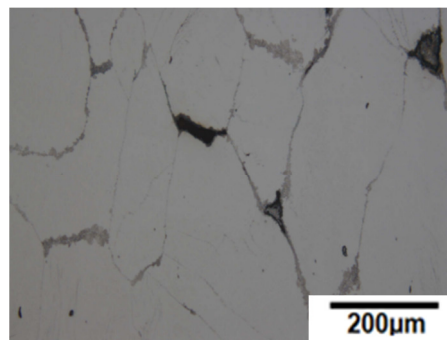
5.2. Comparison with high carbon steel

In the case of high carbon steel, deformed specimens were etched by 2% nital. At 650°C, ferrite/perlite structure was obtained. The ductility in this case shows the smallest RA value in this steel. Very thin ferrite film formed along prior austenite grain boundaries at this temperature. And there are several grain boundary cracks. Microstructure of high carbon steel at 700°C was a (ferrite + perlite)/austenite structure. Thin ferrite and perlite were formed along austenite grain boundaries. Fracture occurred along thin ferrite + perlite along austenite grain boundaries. It is indicating that deformation is localized along prior austenite grain boundaries. Therefore grain boundary separation occurred under this temperature. In contrast, completely ductile fracture was shown in figure 5.3.1 (C) at the 900°C.

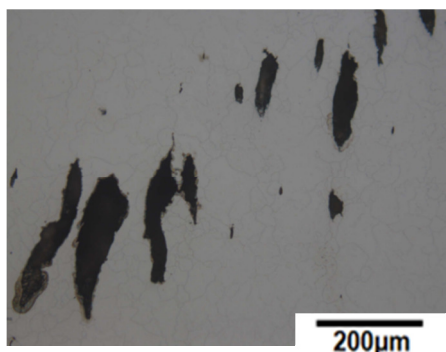




(a) 650 °C



(b) 700 °C



(c) 900 °C

Figure 5.3.1 Room temperature microstructure of steel C cooled from 1200 °C to the deformation temperatures, held during 5s, deformation ($\dot{\varepsilon}=5 \times 10^{-3}$) and finally quenched.

5.3. Growth of α on γ grain on Fe-Si steel

Jin-mo Lee et al., observed $\gamma \rightarrow \alpha$ transformation in an ultralow-carbon steel in detail and found that α grains grow across prior γ grains during $\gamma \rightarrow \alpha$ transformation at the range of the cooling rates in the ultralow-carbon steels(0.5~18°C/s)[24]. Such growth behavior was more marked at lower cooling rates.

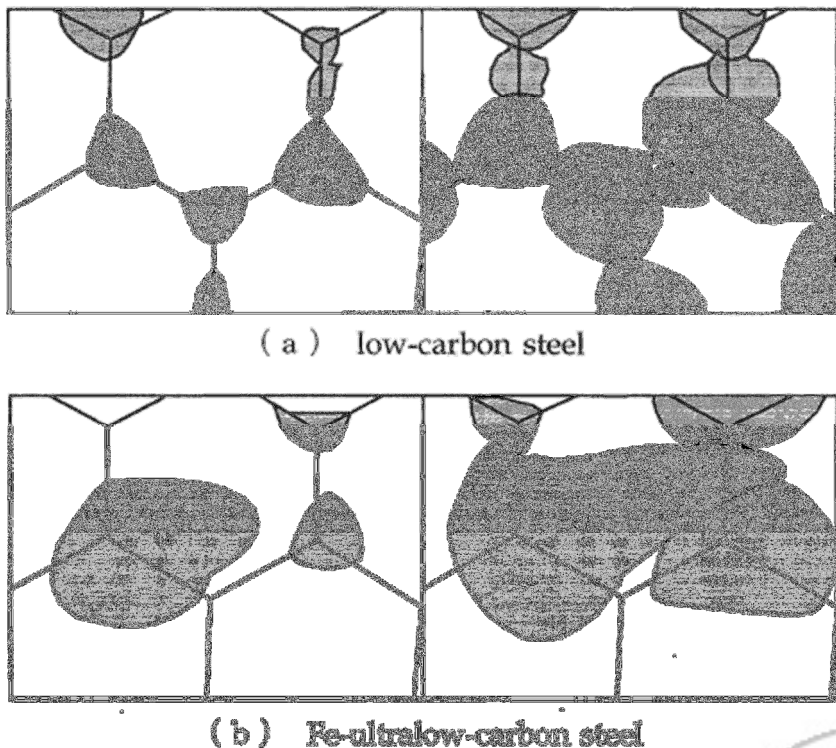


Figure 5.2.1 Schematic diagram comparing growth behavior of α grains between low-carbon and ultralow-carbon steels.[24]

Figure 5.2.1 schematically shows two kinds of growth behavior of α in $\gamma \rightarrow \alpha$ transformation of (a) low-carbon and (b) ultralow-carbon steels. In grains which nucleated mainly on γ grain boundaries and inclusions impinge on each other before crossing the prior γ grains. In ultralow-carbon steels, however, α grains can cross the prior γ grains frequently.

Quantity of carbon in these Fe-Si steels is very similar to the ultralow carbon case. In Fe-Si steel, it is thought that the nucleation rate of α is lower than that in commercial low-carbon steels because the number of precipitates and inclusions is smaller compared to commercial low-carbon steels. Such a low nucleation rate also contributes to the large grain size of α . Furthermore, it is expected that α grains can more easily cross the prior γ grain boundaries in this Fe-Si steels, because impingement effects of precipitates and inclusions are thought to be smaller, although these effects have not yet been clarified by experiments.

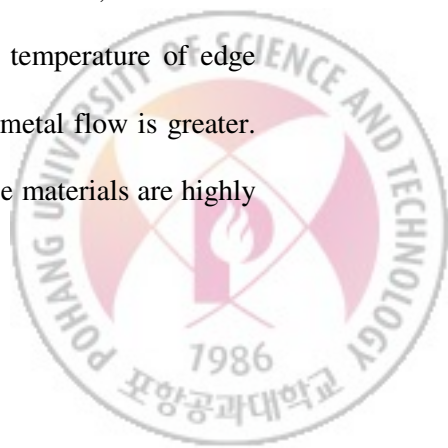
This phenomenon occurred due to extremely low carbon quantity. This kind of transformation is called massive ferrite transformation. Because of this, ferrite was only observed in microstructure.



5.4. Distribution of temperature and strain during hot rolling

The predicted temperature and strain contour at the exit of the roughing mill is presented in figure 4.4.1, 4.4.2, respectively. It can be seen that the extent of the thermally influenced area is edge (~20mm) of the strip. Strain along x-axis is also higher than center of the strip in this region.

The present simulation is capable of prediction phase changes in the strip during hot-rolling process. As mentioned before, the transformation start temperature of steel A is 1013°C. Ferrite can be formed at around austenite grain boundaries after hot-rolling. Therefore, formation of ferrite films played a major role in the loss of ductility during high temperature deformation of Fe-Si steels because concentration of plastic deformation occurs in this region due to the low resistance of ferrite, causing rapid coalescence of microcavities at the austenite/ferrite interface. The loss of ductility of edge within this temperature may be associated with weakening effect on austenite grain boundaries. Moreover, on the surface of center, the metal flow is also restricted by the outer surface, thus, the closer the central part, the greater the resistance, and more difficult the deformation is. Therefore, strain of the center is lower than edge. On the other hand, although the temperature of edge drops rapidly, strain of the edge is higher since the effect of metal flow is greater. Thus, the results presented in this simulation indicate that these materials are highly



susceptible to surface crack on the edge of the strip during hot-rolling processing.



6. Summary and Conclusion

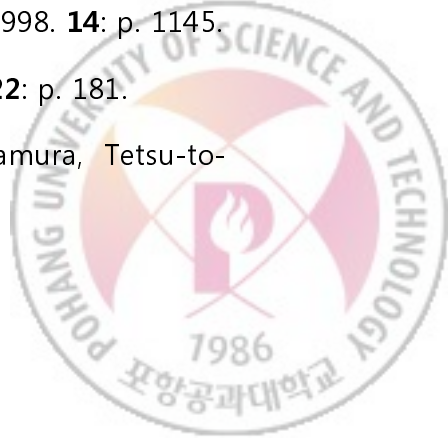
Hot tensile tests were carried out on Fe-Si steels and 0.52C steel and FEM was carried out for calculation of temperature/strain distribution. The conclusions of this study are as follows:

- In the case of Fe-Si steels, results of hot tensile test show that the minimum ductility occurred just below the A_{e3} temperature. Formation of pro-eutectoid ferrite film is an important cause of the ductility in Fe-Si steels during rough mill.
- In the case of 0.52C steel, Formation of pro-eutectoid ferrite film can only partially account for the reduced ductility observed in this steel. But the temperature region of ductility loss is different.
- The results of FEM analysis indicate that
 1. Surface strain was so severe at the edge region.
 2. Temperature of edge surface was decreased under A_{e3} temperature during rough mill.



Reference

1. Jae-Hwa Ryu, B.-H.Y.a.M.-S.C., J.of the Korean Inst. of Met. & Mater., 1998. **36**(6): p. 872.
2. Myung Hwan Han, S.L., Nack J.Kim, Kyung Jong Lee, Taeki Chung, Gwihsan Byun, Mater. Sci . Eng, 1999. **A264**: p. 47.
3. M.shiozaki, M.O., K. Tanaka, T. Shimazu. 1980: United State.
4. J.A.Schey, Jounal of the institute of metals, 1966. **94**: p. 193.
5. J.D.Verhoeven, Fundamentals of Physical Metallurgy, 1975. **1st edn**: p. 352.
6. M.F.Littmann, Metall. Trans. A, 1975. **6A**: p. 184.
7. Schey, J.A., *Workability Testing Techniques*. American Society for Metals Park, Ohio, 1984.
8. Walker, A.J.a.B., *Deformation of Metals During Rolling*. Met. Technol, 1974. **1**: p. 310.
9. Wray, P., Met. Technol, 1981. **8**(12): p. 466.
10. Mintz, B., S. Yue, and J.J. Jonas, International Materials Reviews, 1991. **36**(5): p. 187.
11. D.N. Crowther, a.B.M., Mater. Sci. Technol., 1986. **2**: p. 951.
12. B. Mintz, R.A., and M. Shaker, Mater. Sci. Technol., 1993. **9**: p. 3.
13. MJ Luton, C.M.S., Acta Metallurgica, 1969. **17**(8): p. 1033.
14. A.Cowley, R.A., and B. Minz, Mater. Sci . Tech., 1998. **14**: p. 1145.
15. C.Ouchi, K.M., Trans. Iron Steel Inst. Jpn, 1982. **22**: p. 181.
16. Tadashi Maki, T.N., Naoki Abe and Imao Tamura, *Tetsu-to-Hagane*, 1985. **71**: p. 1367.

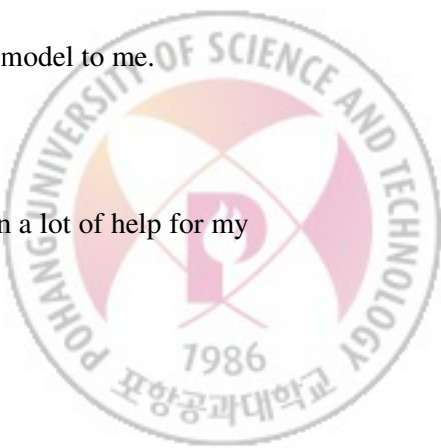


17. Hirowo G. Suzuki, S.N., Jun Imamura and Yasushi Nakamura, Trans. Iron Steel Inst. Jpn, 1984. **24**: p. 169.
18. Ohmori, Y.M.a.Y., MAter. Sci . Eng, 1984. **62**: p. 109.
19. Boelen, A.B.P.C.a.R., Metallography, 1975. **5**: p. 529.
20. al., T.K.e., Kawasaki Steel Technical Report, 1986. **14**: p. 50.
21. Hayashi, M., *Simulation of transverse crack formation on continuously cast peritectic medium carbon steel slabs*. Steel Research.
22. Nicholson, M.E., Trans. TMS-AIME, 1957. **209**: p. 1-7.
23. G. Bernard, J.P.B., B. Condeil and J.C. Humbert, *Rev. Met*, 1978. **78**(467).
24. Jin-mo Lee, K.S., Dentaro ASAKUA and Yasuyuki MASUMOTO, ISIJ International, 2002. **42**(10): p. 1135.

Acknowledgements

First of all, I would like to acknowledge to Professor Yang-Mo Koo who is the director of ATL. With his great support I could finish all these works. It would have been impossible for me to accomplish this thesis without supervision of Professor Jae-Sang Lee. His passion for research is always excellent role model to me.

All members of ATL have offered useful suggestions and given a lot of help for my



work. I particularly thank Myeong-Hoon Kang and Soo-Yeon Lee for giving me technical and theoretical assistance.

Finally, I would love to take this opportunity to thank my family who remained encouraging and full of support.

CURRICULUM VITAE

Name : Bong Guk, Kang



2011 Master Degree

Graduate Institute of Ferrous Technology

Pohang University of Science and Technology

Education :

2009 Bachelor Degree

Mechanical engineering

Inha University

